+ model

ARTICLE IN PRESS

YQRES-02727; No. of pages: 15; 4C:

Available online at www.sciencedirect.com

SCIENCE DIRECT®

ELSEVIER

Quaternary Research xx (2006) xxx–xxx

QUATERNARY RESEARCH

www.elsevier.com/locate/yqres

Late holocene forest dynamics, volcanism, and climate change at whitewing mountain and San Joaquin Ridge, Mono County, Sierra Nevada, CA, USA

Constance I. Millar [a,*], John C. King [b], Robert D. Westfall [a], Harry A. Alden [c], Diane L. Delany [a]

[a] *USDA Forest Service, Sierra Nevada Research Center, Pacific Southwest Research Station, Berkeley, CA 94701, USA*
[b] *Lone Pine Research, Bozeman, MT 59715, USA*
[c] *Smithsonian Institution, Center for Materials Research and Education, Suitland, MD 20746, USA*

Received 17 June 2005

Abstract

Deadwood tree stems scattered above treeline on tephra-covered slopes of Whitewing Mtn (3051 m) and San Joaquin Ridge (3122 m) show evidence of being killed in an eruption from adjacent Glass Creek Vent, Inyo Craters. Using tree-ring methods, we dated deadwood to AD 815–1350, and infer from death dates that the eruption occurred in late summer AD 1350. Based on wood anatomy, we identified deadwood species as *Pinus albicaulis, P. monticola, P. lambertiana, P. contorta, P. jeffreyi*, and *Tsuga mertensiana*. Only *P. albicaulis* grows at these elevations currently; *P. lambertiana* is not locally native. Using contemporary distributions of the species, we modeled paleoclimate during the time of sympatry to be significantly warmer (+3.2°C annual minimum temperature) and slightly drier (−24 mm annual precipitation) than present, resembling values projected for California in the next 70–100 yr.

Keywords: Paleoecology; Medieval climate; Late Holocene; Climate change; Long Valley volcanism; Inyo Craters; Forest history; Paleoclimatic modeling; Tree-ring dating

Introduction

The last millennium is an important reference period for evaluating the significance of future climate change and impacts on ecosystems. The Medieval period (ca. AD 900–1350) in particular has been controversial as an analog for future conditions (Mann et al., 1999; Esper et al., 2002). In the eastern Sierra Nevada, late Holocene climate variability (Stine, 1994; Benson et al., 2002), glacial dynamics (Clark and Gillespie, 1997), volcanism (Sieh and Bursik, 1986), and ecological response (Woolfenden, 1996) are well documented. While the outline of centennial scale variability has been drawn for this region, interactions of forcing factors and ecological disturbance remain poorly understood. Preserved vegetation in the Mammoth Lakes–Long Valley Caldera region provides a detailed record of late Holocene climatic, vegetation, and volcanic dynamics. Scattered across the otherwise barren summits of Whitewing Mtn and San Joaquin Ridge, adjacent to and along the Sierra Nevada crest (Fig. 1), are abundant well-preserved deadwood tree stems (Fig. 2). The stems are, for the elevation, unusually large in diameter and length. The wood is well preserved and in cross-section displays large growth rings. Many stems are stumpless, while others remain rooted but buried in tephra. The summits lie directly adjacent to vents of the Inyo Crater volcanic chain, which has a history of late Holocene eruption episodes (Miller, 1984, 1985; Sieh and Bursik, 1986). The presence of dead trees above current treeline suggests that past climates were different from present, while the proximity of the volcanic vents and condition of the deadwood suggest that an eruption killed the trees.

We undertook this study to evaluate the climatic, ecologic, and disturbance history of the deadwood forest on Whitewing Mtn and San Joaquin Ridge, specifically, to identify species of

* Corresponding author. USDA Forest Service, Sierra Nevada Research Center, Pacific Southwest Research Station, P.O. Box 245 Berkeley, CA 94701, USA (street address: West Annex Bldg., 800 Buchanan St., Albany, CA 94710). Fax: +1 510 559 6499.
E-mail address: cmillar@fs.fed.us (C.I. Millar).

0033-5894/$ - see front matter © 2006 Published by University of Washington.
doi:10.1016/j.yqres.2006.05.001

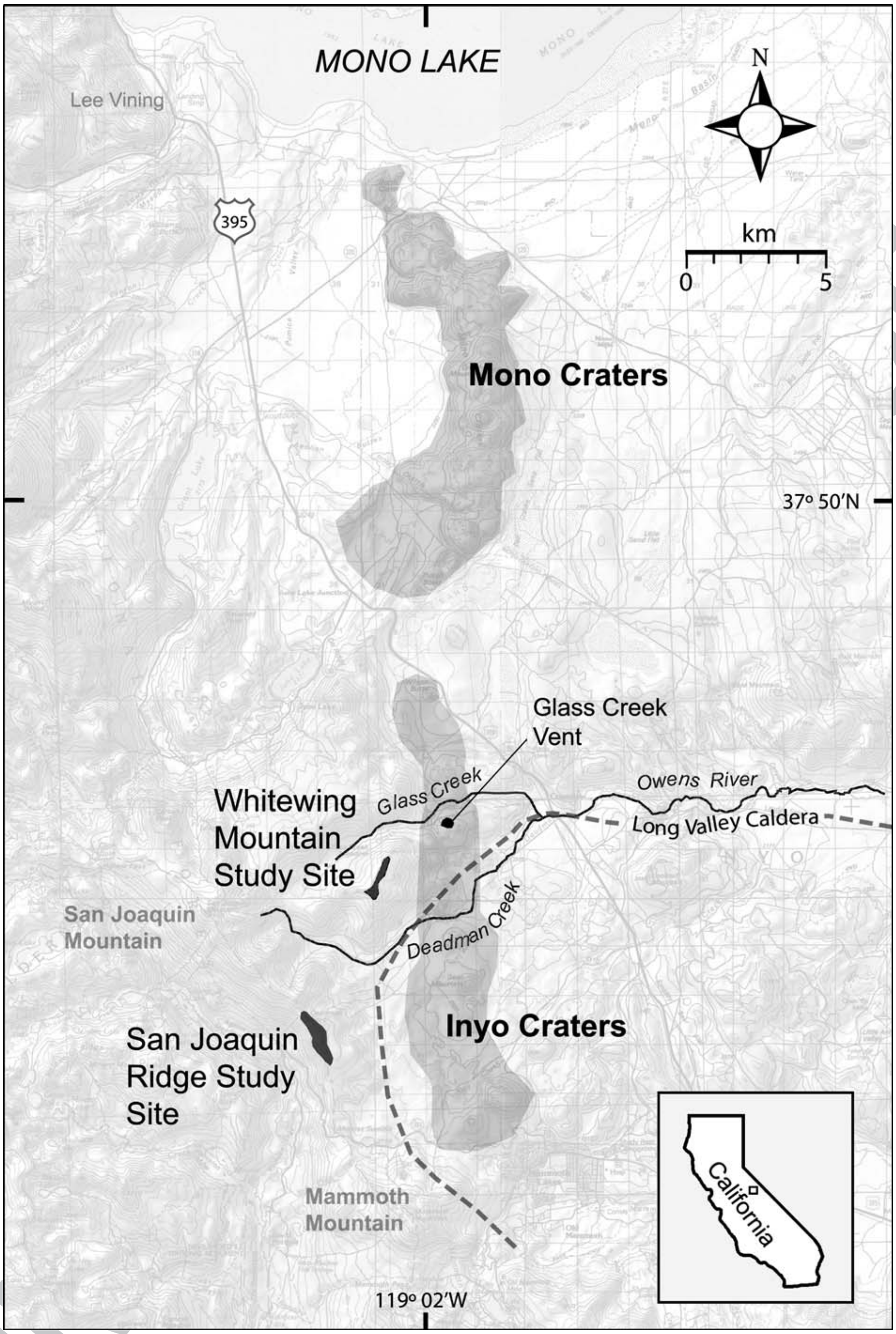

Figure 1. A. Regional map of Whitewing Mtn and San Joaquin Ridge, Mono Co., Eastern Sierra Nevada, CA, showing features mentioned in the text.

trees that grew there, determine tree ages, delimit timing of the Glass Creek eruption, model paleoclimates, and infer causes for the presence and death of the summit forests.

Study area

Location and surficial geology

Whitewing Mtn (3051 m) is a distinct, flat-topped peak that projects eastward from the main crest of the central Sierra Nevada into the headwaters basin of the Owens River (Fig. 1). San Joaquin Ridge (3122 m) forms the Sierra Nevada hydrologic crest west of Whitewing Mtn, creating a low pass at Minaret Summit, 2796 m. Thick deposits of Quaternary tephras dominate all but a few surfaces (Bailey et al., 1976). These derive from eruptions of the adjacent Mono Craters and Inyo Craters, a series of magmatic and phreatic eruptive centers extending from near Mammoth Mtn to Mono Lake (Fig. 1; Wood, 1977). Recent eruptive episodes of vents near Whitewing Mtn occurred 6,000 yr ago, 1250–1400 yr ago, and 550–820 yr ago (Miller, 1984, 1985; Sieh and Bursik, 1986). The most recent eruption of Glass Creek Vent blasted directly onto

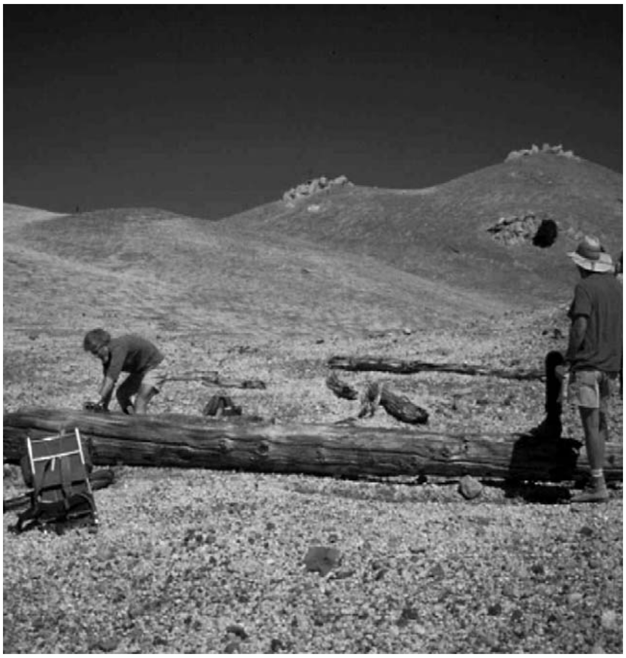

Figure 2. Deadwood stems on Whitewing Mtn, showing flat summit plateau mantled with tephra and scattered large logs.

Whitewing Mtn and San Joaquin Ridge, depositing 8 m of tephra on Whitewing Mtn and 1 m on San Joaquin Ridge (Miller, 1985). Ages for this eruption range from 530 ± 100 cal yr B.P. to 720 ± 60 cal yr B.P., with a minimum tree-ring date of AD 1472 (Wood, 1977; Miller, 1984, 1985). Glass Creek tephra overlies deposits dated 659–737 cal yr B.P. from a nearby phreatic crater on Mammoth Mtn (Sorey et al., 1998).

Current forest types

Plant communities represent typical eastern Sierra elevational zonation, with local variations in extent. Alpine tundra vegetation occurs above 2990 m on San Joaquin Ridge and Whitewing Mtn. Below this is the whitebark pine (*Pinus albicaulis*) forest type, which extends from 2700 m to local treeline at 2990 m. The upper limit of the whitebark type is characterized by a zone of stunted krummholz (shrub-like) pines. This grades into a lower zone of upright pines that form dense clusters and occasionally continuous forest canopies. Outliers occur above the general treeline in sheltered areas around rocky outcrops. Locally, these occur near the summits of Whitewing Mtn and San Joaquin Ridge.

Subalpine forest assemblages overlap the whitebark pine type and extend below it. These vary with slope and aspect as a consequence of ecological tolerances of the species. At the upper elevations are mixed red fir (*Abies magnifica*)/lodgepole pine (*Pinus contorta* ssp. *murrayana*)/mountain hemlock (*Tsuga mertensiana*) forests (2600–2800 m). The extensive cover of red fir is unusual in that the primary species range is west of the Sierra Nevada crest at mid-elevations. This situation appears to result from the low Sierran gap of the San Joaquin Ridge, which provides access for wet Pacific storms to cross the divide, and also serves as a biogeographic corridor. Mixed lodgepole pine/western white pine (*Pinus monticola*) forests grow at 2450–2700 m, and form the lowest of the subalpine types. The subalpine forests grade at lower elevations into lodgepole pine/Jeffrey pine (*Pinus jeffreyi*) forests, which occur from 2300 to 2600 m, and form extensive forests with continuous canopies. Pinyon pine (*P. monophylla*) woodlands form the lowest elevation forest, extending down to 1500 m in the western Great Basin.

Current and paleo-climate

The contemporary climate of the upper Owens River watershed is montane Mediterranean with long dry summers and cool wet winters. Precipitation occurs primarily in winter from Pacific frontal storms that move eastward depositing snow orographically over the western slope of the Sierra Nevada. Gradients of precipitation and temperature are steep, and the eastern slopes and western Great Basin lie in a rain-shadow. Summer moisture occurs sporadically from Gulf-origin monsoon influence. Summer temperatures range from warm/moderate at high elevations to hot east of the crest; atmospheric humidities are low throughout the region.

Late Holocene climates have been described from diverse records in the Sierra Nevada and Great Basin (Woolfenden, 1996; Stine, 1994). The last millennium began with a 450-yr phase that corresponds to the widespread Medieval Climate Anomaly (MCA), and extended from ca. AD 900–1350 in the Sierra Nevada. Proxy records indicate this to have been a dry and warm period, where lake and river levels declined (Yuan et al., 2004; Meko et al., 2001; Stine, 1990, 1994), treelines increased (Graumlich, 1993; Graumlich and Lloyd, 1996), and glaciers retreated (Konrad and Clark, 1998). The MCA was followed by a cool phase coinciding with the northern hemispheric Little Ice Age (LIA), which extended in the Sierra Nevada from AD 1400 to 1900 (Clark and Gillespie, 1997). Closed lake levels remained moderately low, suggesting decreases in effective precipitation and/or runoff relative to present (Stine, 1990). Treeline elevations declined (Graumlich and Lloyd, 1996; Lloyd and Graumlich, 1997) and the largest glacial advances since the Pleistocene are recorded (Clark and Gillespie, 1997). The LIA ended ~ AD 1900; early 20th century proxies record rising temperatures, precipitation increases (Graumlich, 1993) and increasing lake and river levels (Stine, 1990, 1994).

Methods

Stem mapping and stem measurements

We mapped deadwood greater than 1 m length and 10 cm diameter above local treeline on Whitewing Mtn and San Joaquin Ridge between Minaret Summit and Deadman Pass. For each deadwood sample, we measured acropetal orientation of the main stem axis, largest stem diameter, stem length, and noted whether the stem had an attached base (stump). We mapped deadwood by GPS at 17 topographically distinct locations on Whitewing Mtn and 3 locations on San Joaquin Ridge.

Deadwood species identification

We cut transverse sections from deadwood on Whitewing Mtn and San Joaquin Ridge and subsampled these for identification by wood anatomy. Samples represented all major deadwood locations, and included a range of sizes and forms present. Wood samples were prepared for analysis using minor modifications of conventional methods (Kellogg et al., 1982). Samples were identified to generic level using diagnostic keys (Kukachka, 1960) and by comparing unknowns with vouchered material at the Smithsonian Institution's collection, as well as wood from live trees of candidate species collected locally. Identification to species level was critical to our assessment, but difficult with the candidates involved. Thus, in addition to standard keys, we used a combination of specific diagnostic traits to resolve taxonomy, including presence/absence of resin pockets, dimples, crystals in the resin canals, and shape of the ray cross fields (Kellogg et al., 1982; Miller and Wiedenhoeft, 2003; Wiedenhoeft et al., 2003a, 2003b; IAWA, 2004). Resolution of a minimum of six species from Whitewing Mtn (see Results) informed our subsequent methods for dating deadwood and modeling paleoclimates.

Tree-ring dating & analysis

Tree-ring samples were prepared for analysis using standard techniques (Stokes and Smiley, 1968). The Whitewing and San Joaquin Ridge deadwood collection presented challenges for dating as it was characterized by multiple species, low mean growth sensitivity (a measure of high-frequency variation, Fritts, 1976), and relatively short mean ring-series lengths. We modified standard dendrochronological analysis methods (Holmes et al., 1986; Cook and Kairukstis, 1990) in three ways. First, to improve conventional cross-dating graphical methods, we converted measurement series into skeleton plot values using a model derived from an inverse curve relationship:

$$Y = 11.0920 + [(-11.156)/(0.239/X_t)(0.20X_{t-3} + 0.70X_{t-2} + 1.70X_{t-1} + 1.20X_{t+1} + 0.45X_{t+2})]$$

where Y represents the skeleton plot value for a given year, X_t is the ring width for a given year, and $X_{t-3}, X_{t-2}, X_{t-1}, X_{t+1}, X_{t+2}$ are the ring widths for the preceding 3 yr and following 2 yr. Next, we obtained six regional tree-ring chronologies representative of the candidate species from the International Tree-Ring Data Bank (ITRDB, 2005a). From these we determined optimal standardizations for the unknown set (Yamaguchi and Allen, 1992; Yamaguchi, 1994). Finally, using program CRONOL (Cook and Holmes, 1992), we assembled a long reference chronology by combining the tree-ring measurement series of five 1000+ yr high-elevation tree-ring chronologies obtained from ITRDB (ITRDB, 2005b). The unknown samples were combined into a floating chronology that was absolutely cross-dated by correlation and skeleton plot comparison to the assembled reference chronology.

In addition to deadwood, we collected increment cores from 30 live krummholz whitebark pines growing in rocky outcrops below the Whitewing Mtn summit, and dated these with conventional tree-ring techniques.

To compare relative growth conditions of the Whitewing trees to other forests growing in the Sierra Nevada and White Mtns, we extracted data from 40 long tree-ring chronologies from the ITRDB (2005c), computed mean sensitivity values and average ring-width for each, and compared these to Whitewing values.

Dating the glass creek vent volcanic eruption

Previous efforts to date the most recent eruption from Glass Creek Vent relied on radiocarbon assessments of charcoal and minimum tree-ring ages, which yielded a wide age range. Because the trees on Whitewing Mtn and San Joaquin Ridge appear to have been killed by the eruption, their death date should more accurately date the eruption. Scouring winds, however, have eroded unknown numbers of outer growth rings from the samples. We used three independent methods to infer a date for the eruption. First, we searched for deadwood on Whitewing Mtn that was protected from erosion and retained the final year's growth; the most recent death date would estimate the eruption date. Second, we used number of sapwood rings to correct for loss of outer rings from erosion. This assumes that the number of sapwood rings is relatively constant within species at a particular environment. To check this assumption and obtain species-specific values, we surveyed number of sapwood rings in local live trees. For *Pinus albicaulis*, we also had a previous sapwood survey from nearby Yosemite National Park for comparison (King, J.C., unpublished). We then crossdated sapwood boundaries in the deadwood and added the species-specific mean number of sapwood rings derived from the live tree survey to estimate death dates. As a third method, we searched for old trees and deadwood in locations that were topographically protected from the direct volcanic blast, and that might have survived the eruption. In candidates, we inspected ring widths for evidence of extremely suppressed growth during the Medieval period.

Estimating paleo- and current climates at Whitewing Mtn and San Joaquin Ridge

We modeled paleoclimates based on ecological niche theory. The six species that we identified from Whitewing Mtn do not occur together at present. We reasoned that during the period of sympatry on Whitewing Mtn, the climate must have been compatible for all the species, i.e., fundamental niche spaces overlapped (Jackson and Overpeck, 2000). Thus, conditions represented by the intersection of individual climate spaces of the deadwood species would estimate a potential climate of Whitewing Mtn during the time of the summit assemblage. A similar rationale was used by Arundel (2005).

We obtained digitized high-resolution species range maps from the California Gap Analysis Program (Davis et al., 1998) for five of the six deadwood species at Whitewing Mtn (excluding lodgepole pine because of its low habitat sensitivity), and selected each species present in polygons for the dominant and co-dominant, primary through tertiary, cover types in the Sierra Nevada and eastern Sierra eco-regions. The median size of the polygons was 500 ha and minimum resolution 100 ha, which allowed for sensitivity in identifying diverse habitat conditions. We next downloaded 4 km^2 (2.5 arcmin) gridded climate data from PRISM (Daly et al., 1994), extracting layers for annual minimum and annual maximum temperatures; January and July minimum temperatures; January and July maximum temperatures; annual precipitation; and January and July precipitation, for the period of record, 1971–2000. We chose these variables for their ecological significance to the species and because they span annual climatic extremes. The PRISM grids were converted to polygons and sequentially intersected with each of the species' range polygons, with GIS analyses done in ARC/Info (ESRI, 2002).

To determine the overlap among species, we first subjected the merged species-range/PRISM-climate data to discriminant analysis (DA). DA was used because it maximizes differences among groups (species) and discriminates overlap areas better than other methods. A test for normality indicated excessive tailing in the residuals of the DA. Because the large degrees of freedom in our test (>17,000) make this result likely even if the deviation from normality was small, we examined the distribution of our data further. A preponderance of the data closely fit the normal quantile plots, and we concluded that the assumption of normality of residuals in DA was not seriously violated. Using DA, we identified the area of overlap among the five species (JMP, SAS Institute, 2004). We classified the analysis by species with the climatic measures as variables, maximizing multispecies differences in multivariate climate space. The overlapping climate space was defined by those polygons with a Bayesian classification probability greater than 0.09 for all five species. We then computed mean climatic data from the 4 km^2 PRISM model for this classified subset, which we interpret as an estimate of paleoclimate at Whitewing Mtn during the time of sympatry.

To test fit of PRISM data for Whitewing Mtn, we evaluated the root mean square deviation (RMSD) of inferred current climate values from the 1971 to 2000 instrumental records of the Bishop, Lee Vining, Bridgeport, and Bodie, California weather stations (WRCC, 2005). Because RMSDs were large using the 4 km^2 dataset, we sought to improve resolution. Spatial Climate Analysis Service (SCAS, Chris Daly, July 2005) provided us with a new high-resolution dataset (30 arcsec) for the Whitewing Mtn/San Joaquin area for January and July minimum and maximum temperatures, respectively, which we used unadjusted in subsequent analysis.

For the remaining variables, 30 arcsec data were not available from SCAS, so we followed the approach of Hamann and Wang (2005) to develop adjusted high-resolution spatial estimates. For this, we used 30 m digital elevation model (DEM, from Davis

Table 1
Summary statistics of deadwood tree stems on Whitewing Mountain and San Joaquin Ridge

Aspect	*N*	Mean Base[a]	SD Base[a]	Mean Length (m)	SD Length (m)	Mean Dia (cm)	SD Dia (cm)	Stem Orientation[b]
Whitewing Mountain								
SW ridgetop	69	1.68	0.47	4.5	2.1	23.4	12.7	N, NW
SW summit	23	1.57	0.5	3.1	2.2	30.2	12.2	N, NW
NW slope	28	1.82	0.39	3.3	1.7	23.9	10.4	NW, E
Summit plateau	188	1.97	0.16	3.2	1.5	22.1	9.9	E, NE
NW slope	263	1.93	0.26	5.0	2.4	28.7	15.5	SE, N
NW summit	129	1.93	0.26	3.7	1.9	23.6	10.7	N, SE
NW slope, low	64	1.98	0.13	5.4	3.2	31.0	18.0	N, S
NW slope, mid	226	1.99	0.09	4.0	2.3	23.1	10.9	N, E
NW slope, high	78	1.99	0.11	4.0	2.3	26.9	11.7	S, SE
SE slope, high	13	2.00	0.00	3.2	1.6	24.1	13.7	E, SE
SE slope, mid	15	2.00	0.00	4.2	1.8	25.9	6.4	E, NE
E slope, high	166	1.99	0.07	3.7	1.7	22.6	11.4	E, NE
E slope, high	6	2.00	0.00	7.4	2.9	51.3	25.4	E
E slope, high	80	2.00	0.00	3.4	1.6	23.1	10.9	NE, E
E slope, mid	120	1.99	0.09	4.1	2.1	26.7	14.7	E, NE
NE summit	55	1.93	0.20	4.4	2.5	34.0	13.7	NW, NE
N slope	152	1.55	0.50	4.4	2.7	26.7	22.9	S, SE
TOTAL	1675	1.91	0.28	4.1	2.3	26.9	15.0	
San Joaquin Ridge								
S ridgetop	22	1.27	0.46	4.1	1.6	23.1	12.2	SW, S
Central ridgetop	18	1.33	0.49	3.5	1.5	22.4	10.7	SW, W
N ridgetop	20	1.30	0.47	3.7	1.8	23.6	12.7	SW, W
TOTAL	60	1.31	0.46	3.7	1.6	22.9	11.2	

Aspect, number of stems (*N*), condition of stem base (with or without stump attached), mean and standard deviation (SD) stem length and stem diameter (Dia), and primary and secondary orientations (from windrose analysis) are given for deadwood grouped by location on the mountain. The Glass Cr vent is NE-E of Whitewing Mtn and NE of San Joaquin Ridge.

[a] Stem base: 1 = stump attached, 2 = stump absent.

[b] Measured as the direction in which the tree lies from base toward tip.

et al., 1998) tiles for the eastern Sierra Nevada ecoregion, and intersected these with climate data from the PRISM 4 km^2 model (Daly et al., 1994), extracting the PRISM climate data with latitude, longitude, and elevation. We then regressed response-surface equations of latitude, longitude, and elevation of the DEM tiles against the PRISM tiles. Rather than using regression equations of Hamann and Wang (2005), which were based on Canadian locations, we used modified multi-order surface equations of the form: $(\text{latitude} + \text{longitude})^n + \text{elevation} + \text{elevation} \times (\text{latitude} + \text{longitude})^{n-1}$, where >90% fit was obtained when n equaled 5 for the temperature data and 9 for the precipitation data. While this is an overfit as our data are spatially correlated, the high degrees of freedom ensure high fit. As in Hamann and Wang (2005), we took the first derivative for elevation in each equation to estimate lapse rates for climatic data by elevation to adjust temperature and precipitation between the mean elevation of the 4 km^2 PRISM tile for that including Whitewing and the actual elevation for Whitewing. Surface analysis regressions were done in SAS PROC GLM (SAS, 2004) and first derivatives were computed in Mathematica (Wolfram Research, 2004). In nearly all cases, the adjusted data improved fit to the station data relative to the 4 km^2 model. Similar adjustments to PRISM were made to estimate high-resolution current climate for San Joaquin Ridge.

To compare inferred paleoclimate at Whitewing Mtn and San Joaquin Ridge with other locations where the species grow at present we modeled climate at two additional sites: Carson Valley, NV (elev 1701 m), one of the few occurrences of sugar

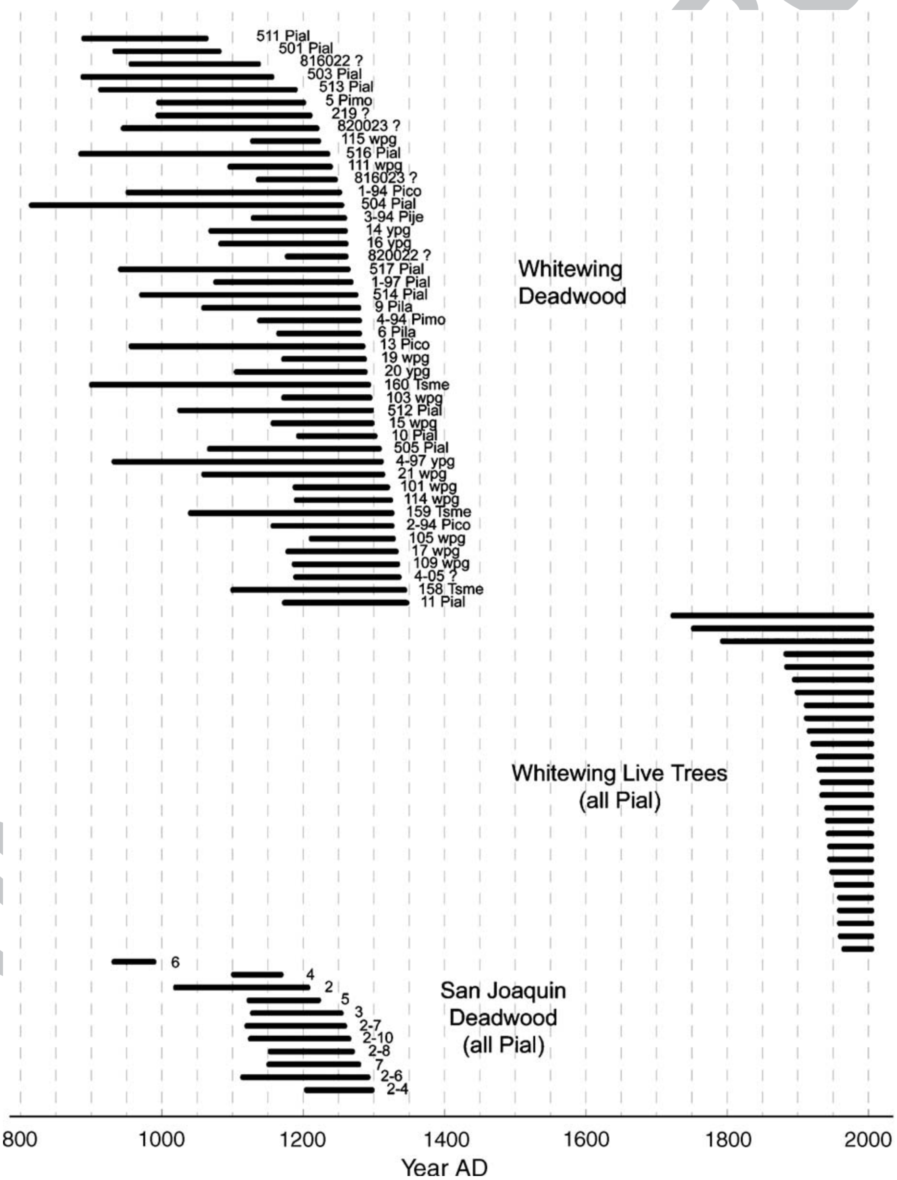

Figure 3. Dated tree-ring series for 45 deadwood samples from Whitewing Mtn, 11 deadwood samples from San Joaquin Ridge, and 27 live stunted trees on Whitewing Mtn. Sample numbers listed next to each series correspond to Appendix 1. For Whitewing, these are *WW* samples, for San Joaquin Ridge, they are *SJR* samples in Appendix 1. Species identifications from wood anatomy are given after the sample number for the Whitewing series, where Pial is *Pinus albicaulis*, Pimo is *P. monticola*, Pila is *P. lambertiana*, Pico is *P. contorta*, Pije is *P. jeffreyi*, and Tsme is *Tsuga mertensiana*, wpg is white pine group and ypg is yellow pine group. A question mark indicates a wood sample whose taxonomic identity could not be determined. All live samples and San Joaquin deadwood samples were *P. albicaulis*.

pine east of the Sierran crest, and Grizzly Peak, Klamath Mtns, northwest California (2059 m), one of the few locations where the six Whitewing deadwood species occur in relatively close association. We estimated the current climate at these locations with the unadjusted 4 km^2 PRISM dataset.

To evaluate the possibility of climatic rather than volcanic cause for forest death on Whitewing Mtn, we extracted from the ITRDB ten high-elevation regional tree rings chronologies growing outside the volcanic influence zone (ITRDB, 2005d), and conducted MANOVA (SAS, 2004) of ring-width between the MCA, LIA, and modern time periods for 25-yr windows throughout the last 1000 yr, and ring-width in the year AD1350 compared to the prior 24 yr. We also computed mean sensitivities of these chronologies to compare against the Whitewing deadwood value.

Results

Deadwood characteristics, stem orientation, and species identification

We mapped and measured 1675 deadwood stems from 17 locations on Whitewing Mtn and 60 deadwood stems from 3 locations on San Joaquin Ridge (Table 1). Most stems on Whitewing Mtn were unrooted and downed, with their basal stumps broken off, while more stems on San Joaquin Ridge retained their stumps. Mean deadwood stem lengths and diameters respectively were 4.1 m and 26.9 cm on Whitewing Mtn, and 3.7 m and 22.9 cm on San Joaquin Ridge. Based on windrose summaries, the predominant orientation of downed stems was north to east on Whitewing Mtn, and southwest to west on San Joaquin Ridge (Table 1).

Taxonomic identifications from deadwood anatomy were made on 78 samples from Whitewing Mtn and 17 from San Joaquin Ridge (Appendix 1). Diagnostic traits allowed explicit identification of six species on Whitewing, including 42 *Pinus albicaulis*, 5 *P. lambertiana*, 11 *P. monticola*, 3 *P. contorta*, 2 *P. jeffreyi*, and 6 *Tsuga mertensiana* samples. Seven additional samples were identified to a yellow-pine group, which includes *P. jeffreyi*, *P. contorta*, and *P. ponderosa*, and 2 additional samples to a white pine group, which includes *P. monticola*, *P. flexilis*, and *P. lambertiana*. Twenty-nine samples were rooted buried stumps and represented the taxonomic diversity of the total collection. All samples from San Joaquin Ridge were *P. albicaulis*.

Deadwood stem ages and dates

We processed 85 deadwood samples from Whitewing Mtn and 25 from San Joaquin Ridge for cross-dating. Of these we determined explicit calendar dates for 45 samples from Whitewing Mtn and 11 from San Joaquin Ridge (Fig. 3). Whitewing Mtn samples had an average series length of 165 yr, mean sensitivity of 0.171, and average ring width of 0.85 mm. Dates for the oldest (innermost) rings ranged AD 815–1211, and youngest (outermost) rings ranged 1063–AD 1350. Samples of all species were well represented throughout the period with no temporal gaps in the record. The San Joaquin Ridge samples had an average series length of 121 yr and spanned the period AD 925–1298, with a 31 yr gap, AD 989–1019.

Live krummholz whitebark pines sampled in rock outcrops below the summit of Whitewing Mtn had an average series length of 86 yr. The oldest sample dated to AD 1723. Three trees were over 200 yr old; the remaining 24 samples were less than 120 yr old (Fig. 3).

Dating the glass creek vent eruption

We were successful in applying three independent methods to corroborate a date for the Glass Creek Vent eruption. Although wind erosion removed rings from the outer circumferences of most deadwood samples on Whitewing Mtn and San Joaquin Ridge, we found one sound stem that retained its outer bark edge and had the youngest date of all samples. Sample WW11, a rooted *P. albicaulis* stem, had a branch knot

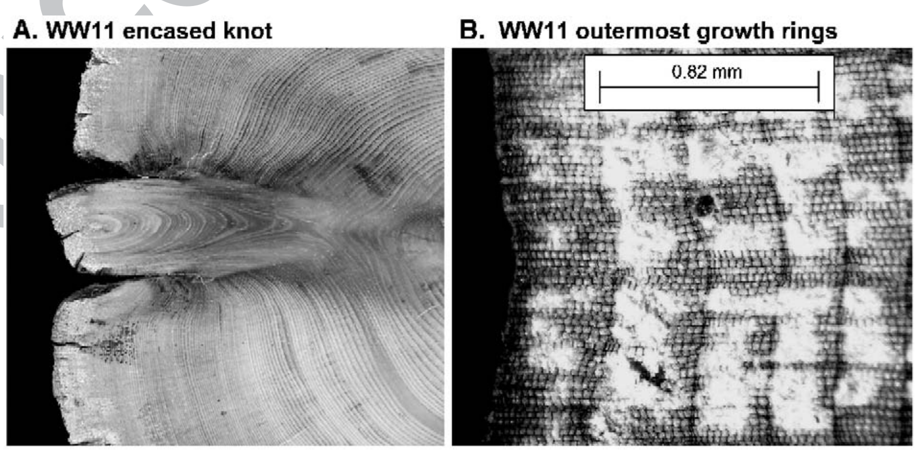

Figure 4. Cross-sections of Whitewing sample WW11, *Pinus albicaulis*, whose outer growth ring was protected from erosion by a dead knot. The outermost ring dates to AD 1350 and lacks the final cells of the growing season, suggesting that the tree died near the end of the growing season (late summer) AD 1350 in the Glass Creek eruption. (A) Stem cross-section showing the protected outer rings growing in the dead knot cavity and the outer stem (waney) edge. (B) Magnification of the outermost growth rings showing the incomplete final ring lacking the typical terminal small cells.

Table 2A
Sapwood surveys in live trees and sapwood dating in deadwood samples

Survey of Sapwood Rings in Live Trees			
Species	*N*	Mean number Sapwood Rings	Standard deviation
Pinus albicaulis (YNP)	181	63.5	15.7
Pinus albicaulis (GC)	42	61.2	18.0
Pinus albicaulis (all[a])	223	63.0	16.2
Pinus flexilis	96	70.2	17.5
Pinus monticola	24	45.3	15.9
Pinus contorta	30	88.2	22.5
white pine group[b]	120	65.2	19.8

Results from a survey of number of sapwood rings in live trees from Yosemite National Park (YNP) for *Pinus albicaulis*) and the Glass Creek Watershed (GC) for all species.
[a] Combined dataset from YNP and GC samples.
[b] Dataset derived by merging values from *P. flexilis* and *P. monticola* samples.

embedded in the main stem. The branch died before the main stem, creating a knot cavity that protected the bark and outer rings of the main stem (Fig. 4A). The ring series of the lower main stem dated AD 1052–1187; the protected stem series in the knot cavity overlapped this by 10 rings and had an inner date of AD 1177. The terminal (outer) ring dated to AD 1350 and appeared incomplete (Fig. 4B). This ring appeared to lack the narrow latewood cells that typically signify the end of the growing year. We estimated the death date of this sample as late summer AD 1350, and propose this as the eruption date.

Thirteen deadwood samples from Whitewing Mtn had dateable heartwood/sapwood boundaries, including six whose boundaries dated to the late 13th century. Using species-specific values from our survey of 343 live local trees (Table 2A), we estimated death dates for the six deadwood series. The range of mean dates using this method was AD 1322–1370 with 95% confidence intervals extending the range to AD 1290–1414 (Table 2B).

During an extensive study of forest dynamics in Glass Creek watershed, we found only one deadwood sample whose ring series extended through AD 1350. Sample GC 7/13/98-1 was an upright, rooted stump, 107 cm in diameter, buried in coarse

Table 2B
Sapwood surveys in live trees and sapwood dating in deadwood samples

Estimates of death dates in Whitewing Mtn deadwood samples					
Whitewing Sample ID	Species ID[a]	Pith yr AD	Outer Ring yr AD	Sapwood Boundary yr AD	Estimated Death Mean and CI, yr AD
WW505	Pial	1067	1308	1259	1322 (1290–1354)
WW17	wpg	1178	1332	1282	1347 (1308–1386)
WW105	wpg	1211	1328	1283	1348 (1309–1387)
WW113	wpg	1190	1324	1289	1354 (1315–1393)
WW 109	wpg	1187	1334	1292	1357 (1318–1396)
WW2	Pico	1157	1326	1282	1370 (1326–1414)

Sapwood boundary dates and estimates of death dates for six deadwood Whitewing Mtn samples. Death dates are calculated by adding the species or group mean number of sapwood years from the surveys of local live trees to the date of deadwood sapwood–heartwood boundaries. Pith dates are dates of tree birth; death dates are given by mean year with 95% confidence-interval ranges. The resulting range of death dates corroborates the eruption date inferred from other methods (AD 1350).
[a] Pial is *Pinus albicaulis*; Pico is *Pinus contorta*; wpg is white pine group.

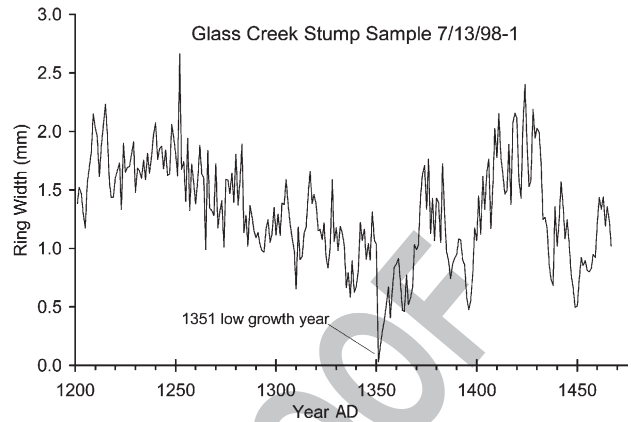

Figure 5. Ring-width trace from deadwood stump sample GC 7/13/98-1, putatively identified as *Pinus contorta*, growing at 2081 m elevation in Glass Creek watershed. This tree survived the AD 1350 eruption, presumably due to its protected location, but shows severely depressed growth during the following growing season and in the subsequent year (AD 1351 and 1352 , respectively), corroborating the estimated date for the eruption.

tephra. The sample was located at 2801 m in a narrow col 1.5 km west of the Whitewing summit; wood anatomy indicates it is lodgepole pine. The stem date range was AD 1201–1467. The AD1350 growth ring (1.068 mm) is near-average width (1.310 mm), but ring AD1351 is highly suppressed (0.030 mm) and comprises only 1–2 cells (Fig. 5). Ring AD1352 is also very narrow (0.162 mm).

Current and paleo-climate at Whitewing Mtn and San Joaquin Ridge

The first two canonical vectors of the discriminant analysis accounted for 97% of the differences in current climate space of the five deadwood species on Whitewing Mtn as estimated from

Table 3
Canonical discriminant analysis of the differences in contemporary climate space for distributions of *P. albicaulis*, *P. monticola*, *P. lambertiana*, *P. jeffreyi*, and *P. contorta* in the Sierra Nevada and western Great Basin

(A) Summary		
	Canonical vector 1	Canonical vector 2
Correlation	0.76	0.45
Percent	81	16
(B) Individual correlations		
	Correlations	
Annual max temp	0.95	−0.17
Annual min temp	0.95	−0.05
Annual precipitation	0.18	0.92
January max temp	0.92	−0.29
July max temp	0.89	0.13
Jan min temp	0.90	0.24
July min temp	0.80	0.06
Jan precipitation	0.22	0.92
July precipitation	−0.58	0.07

(A) Overall correlation of climate variables to first two canonical vectors and percent of variation explained by first two canonical vectors. (B) Correlations of individual climate variables to first two canonical vectors.

their current Sierra Nevada distribution and PRISM climate model (Table 3). The first vector showed the greatest difference among species, accounting for 81% of the differences. Temperature variables were strongly correlated with scores on this vector, and precipitation, excepting July precipitation, was strongly correlated with the second vector. July precipitation was negatively correlated with the first vector. Scatter diagrams from discriminant analysis for the individual species indicate differences in climate space among the species (Figs. 6A–E); the greatest difference was between whitebark pine and sugar pine. From the values for the mean overlap among the five species (Fig. 6F), we estimated mean values for six temperature and three precipitation variables (Table 4), which we propose reflect a potential paleoclimate on Whitewing Mtn during the time the species co-occurred. With the exception of minimum temperatures, RMSDs were less than 15% of the station means, and all RMSDs were equal to or less than those reported in Hamann and Wang (2005).

The paleoclimate modeled for Whitewing during the Medieval period was significantly warmer and slightly drier than present (Table 4). Medieval mean annual minimum temperature was warmer than current by 3.2°C, with large differences in winter (+3.5°C, January) and summer (+4.0°C, July). Mean annual maximum temperature was also greater in the Medieval period (+2.3°C), with greater differences in winter (+3.2°C, January) than summer (+2.6°C, July). Annual precipitation was less by 24 mm. The modeled Medieval climate for Whitewing Mtn compared closely with current conditions estimated from PRISM for the Carson Range extant sugar pine location, 200 km distant from Whitewing Mtn and 1350 m lower, and for the Grizzly Peak mixed conifer stand, 580 km distant and 992 m lower.

Our analyses of mean ring-widths and mean sensitivities from the Whitewing Mtn series relative to other regional chronologies indicated little evidence for climatic rather than volcanic cause of death. Compared to 40 long regional tree-ring chronologies, mean sensitivity of the Whitewing set ranked

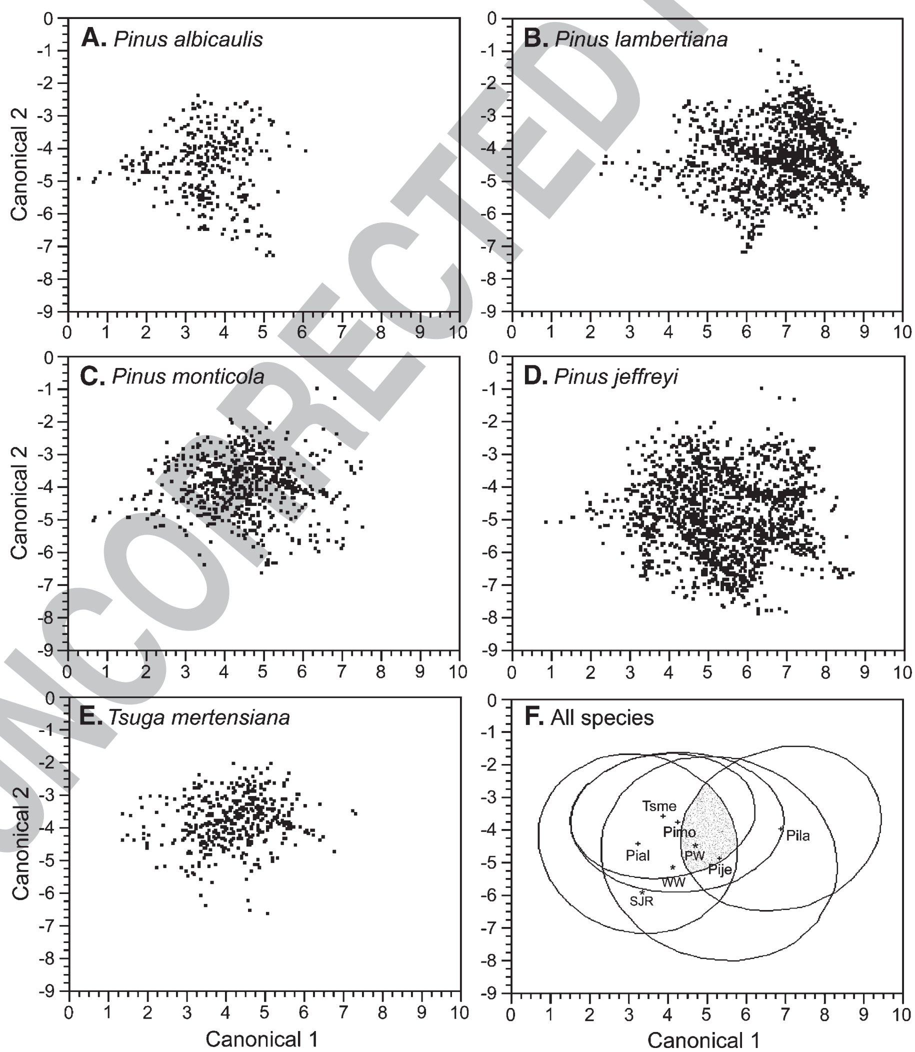

Figure 6. Scatter diagrams of discriminant analysis scores for Sierra Nevada/western Great Basin species distribution ranges. Each point is an individual polygon from the Sierra Nevada GAP range dataset. (A) *Pinus albicaulis* (Pial), (B) *P. lambertiana* (Pila), (C) *P. monticola* (Pimo), (D) *P. jeffreyi* (Pije) and (E) *Tsuga mertensiana* (Tsme). (F) All species. Circles representing 90% of the discriminant values for each species show overlap among species (shaded), the mean of which was modeled to estimate climate at time of species sympatry (paleoclimate of Whitewing, PW); centroids for each species are indicated. Current climate points for Whitewing Mtn (WW) and San Joaquin Ridge (SJR) are indicated.

Table 4
Current and paleohistoric climate estimates for Eastern Sierra Nevada as modeled and adjusted from PRISM climate model (Daly et al., 1994) and discriminant analysis

Location	Ann ppt (mm)	July ppt (mm)	Jan ppt (mm)	Ann min temp (°C)	Jan min temp (°C)	July min temp (°C)	Ann max temp (°C)	Jan max temp (°C)	July max temp (°C)
(A) Current climate: 1971–20AD 00									
Carson Range, NV (e Sierra sugar pine stand)	972	16	153	−0.5	−7.2	8.0	13.1	4.0	24.3
Grizzly Peak, NW CA (6 species growing in near-sympatry)	959	15	178	0.4	−5.1	7.5	15.6	4.4	27.9
San Joaquin Ridge	945[a]	5[a]	195[a]	−4.5[a]	−9.8[b]	3.4[b]	10.9[a]	0.7[b]	21.2[b]
Whitewing Mtn	1064[a]	14[a]	184[a]	−3.7[a]	−10.0[b]	3.6[b]	11.0[a]	1.4[b]	21.5[b]
(B) Paleoclimate: AD 800–1350									
Whitewing Mtn	1040	13	186	−0.5	−6.5	7.6	13.3	4.6	24.1
(C) Difference in Whitewing Mtn Climate Values									
Paleo-Current	−24	−1	+2	+3.2	+3.5	+4.0	+2.3	+3.2	+2.6
(D) Deviations of PRISM estimates from instrumental station records									
RMSD/Mean	0.04[a]	0.13[a]	0.05[a]	0.44[a]	0.52[b]	0.56[b]	<0.01[a]	0.03[b]	0.01[b]

(A) Current climate estimates for four locations: Carson Range, NV location of extant eastern Sierra sugar pine (1350 m below Whitewing Mtn summit); Grizzly Peak, northwest CA location of near-sympatric extant occurrence of six Whitewing deadwood species (992 m below Whitewing Mtn summit); Whitewing Mtn,; and San Joaquin Ridge. Estimates based on period-of-record 1971–2000 and 4 km^2 PRISM model except January and July minimum and maximum temperatures, respectively, which are based on 30 arcsec PRISM model; for Whitewing and San Joaquin Ridge, PRISM estimates of precipitation, annual minimum and annual maximum temperatures are adjusted for elevation at 30 m intervals. (B) Paleoclimate values estimated from 4 km^2 PRISM model based on the mean jointly classified observations derived from discriminant analysis of multi-species climate space using five deadwood species present on Whitewing Mtn and dating to AD 800–1350. (C) Differences in climate values for Whitewing Mtn between time periods (Paleoclimate-Current Climate). (D) Root mean squared deviations (RMSD)of adjusted PRISM estimates from the instrumental records for four weather stations (Bishop, Lee Vining, Bridgeport, and Bodie CA, WRCC, 2005), based on equivalent periods-of-record (1971–2000).

[a] Estimates adjusted from the 4 km^2 PRISM model for elevation at 30 m intervals.

[b] Estimates based on unadjusted 30 arcsec PRISM estimates.

fourth from the lowest, similar to values from mid-elevation (1800–2200 m) mesic, westslope chronologies, and significantly lower than means from subalpine forests growing at elevations comparable to Whitewing Mtn. Relative to ten high-elevation regional chronologies, mean sensitivities of the Whitewing set were not significantly greater during the mid-1300s relative to a reference of AD 1300–1500 ($P < 0.001$). Similarly, although mean ring-width for the period AD1325–1350 was less than during AD 1300–1325, it was significantly greater than means for all 25-yr periods during four centuries of AD1450–1850 ($P < 0.001$). Ring-width during the year AD1350 for the ten high-elevation chronologies (from outside the volcanic influence zone) was greater, though not significantly ($P > 0.07$) than the mean during the previous 24 yr.

Discussion and conclusions

Deadwood forest composition and age

The abundant deadwood on Whitewing Mtn and San Joaquin Ridge was extremely well preserved, enabling taxonomic identification to species level with high confidence. Diagnostic traits readily distinguished the samples to two genera, *Tsuga* and *Pinus*. Only one hemlock species (*Tsuga mertensiana*) is currently native to the Sierra Nevada, and we assume this to be the Whitewing taxon. Diagnostics readily separate the subgenera within *Pinus*. Within subgenus Diploxylon, *P. contorta* is distinguishable from taxa within subsection *Ponderosae*. We assume the yellow pine group to be represented by Jeffrey pine and not Ponderosa pine (*Pinus ponderosa*) because the latter grows at distant, low, westslope, elevations in the Sierra. It remains, however, a candidate. Within subgenus Haploxylon, species-specific diagnostics distinguished whitebark pine and sugar pine, while western white pine and limber pine were difficult to separate and identification depended on sample quality.

The identification of six conifer species growing together in forest stand conditions at elevations above 3000 m on Whitewing Mtn was an unexpected finding from our study. The possibility that the stems did not originate from trees growing on the summit, rather were transported upslope by a volcanic blast from lower elevation forests, is counter-indicated by the presence of rooted stumps representing the range of species on the summit plateau. Only whitebark pine currently occurs at similar elevations elsewhere in the Sierra Nevada, although usually in krummholz form and a few clusters of krummholz whitebark pine currently occur in protected rock outcrops on the slopes of Whitewing Mtn and San Joaquin Ridge. The deadwood stems, by comparison, are scattered widely on the summit plateau and slopes, have long, straight stems and relatively large diameters, indicating a tall forest structure.

Lodgepole pine and mountain hemlock are currently at the elevation of Whitewing Mtn elsewhere in the Sierra where conditions are protected. In windy, exposed locations mountain hemlock rarely occurs at this elevation, and lodgepole pine is usually stunted. These species currently grow in straight-stem condition more than 200 m below the summit of Whitewing

Mtn. Western white pine is a common but sparsely distributed species of the upper montane zone in the eastern Sierra. In the region of Whitewing Mtn, it occurs mixed with other pines on the slopes of Whitewing Mtn and San Joaquin Ridge more than 250 m below the summits. Jeffrey pine is locally abundant in this region more than 400 m below the Whitewing summit.

An especially surprising identification from Whitewing Mtn was sugar pine. This species is typical of low- to mid-montane, mesic habitats of southern Oregon to northern Baja California (Critchfield and Little, 1966). In the Sierra Nevada, sugar pine is a component of the west-slope mixed-conifer forest, and extends 610–2285 m (Kinloch and Scheuner, 1990). Occasional outliers occur higher, and the nearest native sugar pine to Whitewing Mtn occurs west of the Sierra crest in the upper watershed of the Middle Fork San Joaquin River, 25 km distant and ~700 m below Whitewing Mtn (Griffin and Critchfield, 1976). The closest occurrence east of the Sierra crest is in Alpine County, 100 km northwest and 1150 m lower than Whitewing (Griffin and Critchfield, 1976).

The identification of sugar pine in the Whitewing area is supported by independent evidence: (1) several wood samples from Whitewing Mtn, first discovered in the late 1970s, were sent to two wood identification laboratories, both of which reported the samples as sugar pine (1980, letters on file from Forest Products Lab, Madison, WI and University of California Forest Products Lab, Richmond CA); (2) wood from Inyo Craters tephra soil horizon, extracted from a roadcut near Deadman Creek, was noted without documentation as sugar pine (Stine et al., 1984); (3) anecdotal reports from a Bishop, CA woodsworker detail the “last old-growth sugar pine” having been sawn from the upper Dry Creek watershed, adjacent to San Joaquin Ridge in the mid 1940s (1995 unpublished oral history report on file, USFS, Bishop, CA). No live native sugar pine is known from this region at present, despite extensive field surveys.

The species diversity, short ring-series length, and complacent nature of growth in the Whitewing Mtn samples initially made cross-dating difficult. Our approach, using multiple methods and cross-checking each preliminary date, provided a final set of dates for Whitewing and San Joaquin samples whose accuracy has high confidence. The diversity and number of samples spanned the Medieval period and dated AD 815–1350 with no indication of older samples. This suggests the forest established rapidly, and possibly the earliest trees colonized the summit after a previous eruption of the Inyo Craters.

Age of the glass creek vent eruption

The end of the Medieval forest on Whitewing Mtn appears to have resulted from a volcanic eruption at Glass Creek Vent, as indicated in several ways. First, the slope of the outer ring dates in the Whitewing series is steep (Fig. 3) and, allowing for variable wood erosion, suggests that that the trees died synchronously. If the trees had been experiencing increased environmental (fire or insect) or climatic (drought) stress, the ring widths in the early–mid 1300s would be expected to decrease and mean sensitivities increase. We found, to the contrary, no significant differences in mean sensitivities in the Whitewing samples over time nor evidence in other regional high-elevation forests for stress in this period. To the contrary, evidence points to favorable growth conditions during the early–mid 1300s. Similarly, no evidence indicates that, prior to late summer, the year AD1350 was anomalously stressful. Only in AD1351 at Whitewing Mtn was an unprecedented growth depression obvious. Considered together, the evidence points to volcanic eruption as the cause of forest death on Whitewing Mtn, not other environmental or climatic stress. Based on stem orientations, it appears more likely that the eruption killed the trees, which later blew down in winds or fell along slope gravity, rather than were broken directly by the volcanic blast.

Our three independent methods corroborate an eruption date of Glass Creek Vent as late summer AD 1350. This estimate falls in the range previously indicated by radiocarbon and minimum tree-ring methods (Miller, 1984, 1985; Sieh and Bursik, 1986; Sorey et al., 1998). A fourth line of evidence for this date comes from tree-ring series dates of dead and live limber pine 0.5 km north of the Whitewing summit (Millar, C.I., manuscript in preparation), which we dated as continuous from 1362 BC to AD 1339, a gap for 52 yr, then a continuous record from AD 1392 to the present.

Paleoclimate, current and future climates

The range of dates for the deadwood samples, AD 815–1350, coincides with the period identified from multiple proxies in the Sierra Nevada and western Great Basin as the Medieval Climate Anomaly. This period overlaps nearly exactly two regional centennial-scale droughts, dated AD 900–1112 and AD1200–1350, identified from lowered lake and river levels (Stine, 1990, 1994). Extensive drought during the Medieval period has been further interpreted from lake sediments (Yuan et al., 2004; Benson et al., 2002; Li et al., 2000; Kleepe, in press), tree-ring reconstructions (Meko et al., 2001), and glacial records (Konrad and Clark, 1998). Tree-ring reconstructions indicate increased temperature relative to present (Graumlich, 1993; Scuderi, 1993) and higher treelines (Graumlich and Lloyd, 1996; Lloyd and Graumlich, 1997), and pollen reconstructions show greater abundance of fir in high-elevation communities than at present (Anderson, 1990).

The ecologic patterns and climatic estimates at Whitewing and San Joaquin Ridge corroborate studies showing significant Medieval warmth in the California region but provide evidence for differences between high and low elevations in moisture availability. Whereas mid-low elevations in the Sierra Nevada experienced extreme Medieval drought, precipitation at Whitewing appears to have been adequate to support mesic-adapted species. Excessive temperatures at low-mid elevations would force montane conifers uphill where temperatures were moderate. In contrast to lower elevations, however, high plateaus and summits of the eastern Sierra appear to have retained relatively more precipitation due to mountain meteorological processes that favor orographic precipitation in winter and summer convective moisture. Further, the locations of the study sites relative to the low Sierran divide along San Joaquin Ridge positioned them to capture more precipitation from Pacific storms than other eastside locations. Thus, even while severe drought was experienced at lower elevations, the high elevation and position of Whitewing received adequate precipitation capable of supporting mesic and warm adapted species.

That the Medieval forest on Whitewing was growing under mild, favorable conditions (warm with adequate moisture) is further indicated by extremely low mean sensitivities and large average ring widths. These variables reflect relative tree health and growth in that larger ring width and lower mean sensitivity values occur when trees grow under less limiting environmental conditions. As indicated by our comparison of the Whitewing dataset with 40 regional chronologies, mean sensitivities as low as the Whitewing deadwood set rarely occur in trees growing in subalpine conditions, where physical stress dominates interannual ring variability, and mean sensitivities typically range above 0.3. The similarity of climates at the extant eastside sugar pine stand in the Carson Range, NV and the mixed conifer stand at Grizzly Peak, northwest CA to the modeled paleoclimate for Whitewing Mtn is additional support for an interpretation that the conditions at Whitewing were warm but not excessively dry.

A projection of warm Medieval temperatures with only small decreases in precipitation at high elevations is not inconsistent with extreme drought at lower elevations indicated by other studies. Warm winter temperatures would result in significantly reduced winter snowpack, early run-off, lengthening of the Mediterranean summer drought, and reduced available moisture. This situation resembles 20th–21st century trends in the Sierra Nevada, where increasing minimum temperatures, especially in winter, are reducing snowpack accumulation, accelerating early run-off, and leading to effective drought during the spring-fall growing season despite lack of annual average decrease in precipitation (Dettinger et al., 2004). The modeled Whitewing Medieval climate closely compares to climate projections for California in AD 2070–2099 (Hayhoe et al., 2004). In that study, average temperature increases of 2.3–5.8°C were projected and slight increases or decreases in precipitation (+38 mm to −157 mm). Coupled vegetation–climate projections for 2070–2099 inferred significantly reduced spring snowpacks and earlier runoff. Based on those conditions, Hayhoe et al. (2004) estimate 75–90% reduction in California subalpine forest by AD 2070–2099. Recognizing significant CO_2 differences between future projected and Medieval climates, our empirical findings of significant increase in subalpine forest extent and diversity during similar climate conditions nonetheless raise questions about modeled results of future forest reductions in the subalpine zone. As we have observed for the 20th century, subalpine forests in the Sierra Nevada often respond non-linearly with increasing temperature, showing abrupt changes and reversals (Millar et al., 2004). Such trends may well ensue under future warming.

Acknowledgments

We thank Chris Daly, William Evans, Andreas Hamann, Dave Hill, Stephen Gray, Robin Tausch, Alex Wiedenhoft, and an anonymous reviewer for critical discussion and reviews of the manuscript; Chris Daly for offering new high-resolution PRISM data; Veronique Greenwood and Karolyn Wyneken for field assistance; Jim Jensen, Tom Higley, and Wally Woolfenden for early reconnaissance work, and the NOAA World Data Center for Paleoclimatology, International Tree-Ring Data Bank, for providing tree-ring chronologies.

Appendix A. Locations and descriptions of deadwood trees stems sampled for species identification from wood anatomy on Whitewing Mountain and San Joaquin Ridge

Samples indicated as dated are graphed in Figure 3

Sample ID	Stem Length and Diameter[a]	Condition	Stump	Dated?	Species ID[b]
Whitewing Mountain-North Slope:					
WW1–97	9 m, 20 cm	upright stem	rooted	yes	*Pinus albicaulis*
WW2–97	12 m, 91 cm	downed log	absent	no	*Tsuga mertensiana*
WW3–97	1 m, 35 cm	upright stem	rooted	no	*P. albicaulis*
WW4–97	12 m, 81 cm	downed log	absent	yes	yellow pine grp
WW158	5 m, 55 cm	downed log	absent	yes	*T. mertensiana*
WW159	3 m, 20 cm	downed log	absent	yes	*T. mertensiana*
WW160	7 m, 40 cm	downed log	absent	yes	*T. mertensiana*
WW161	8 m, 40 cm	upright stem	rooted	no	*P. albicaulis*
WW510–98	3 m, 23 cm	upright stem	rooted	no	*P. albicaulis*
WW511–98	1 m, 20 cm	upright stem	rooted	yes	*P. albicaulis*
WW512–98	2 m, 25 cm	downed log	absent	yes	*P. albicaulis*
WW513–98	4 m, 31 cm	upright stem	rooted	yes	*P. albicaulis*
WW514–98	3 m, 40 cm	upright stem	rooted	yes	*P. albicaulis*
WW515–98	3 m, 35 cm	downed log	absent	no	*P. albicaulis*
WW516–98	1 m, 33 cm	upright stem	rooted	yes	*P. albicaulis*
WW517–98	3 m, 40 cm	upright stem	rooted	yes	*P. albicaulis*
Whitewing Mountain–Northwest Slopes and NW Summit:					
WW 200	1 m, 28 cm	rooted stump	present	no	*P. albicaulis*
WW201	0.5 m, 28 cm	rooted stump	present	no	*P. monticola*
WW202	0.3 m, 27 cm	rooted stump	present	no	yellow pine grp
WW203	0.6 m, 20 cm	rooted stump	present	no	*P. albicaulis*
WW204	0.6 m, 15 cm	rooted stump	present	no	*P. albicaulis*
WW206	0.7 m, 28 cm	rooted stump	present	no	*P. monticola*
WW207	0.1 m, 22 cm	rooted stump	present	no	*P. lambertiana*

(continued on next page)

Appendix A (*continued*)

Sample ID	Stem Length and Diameter[a]	Condition	Stump	Dated?	Species ID[b]
Whitewing Mountain–Northwest Slopes and NW Summit:					
WW208	0.2 m, 31 cm	rooted stump	present	no	*P. monticola*
WW209	0.2 m, 31 cm	rooted stump	present	no	*P. albicaulis*
WW210	0.2 m, 31 cm	rooted stump	present	no	*P. albicaulis*
WW211	0.4 m, 21 cm	rooted stump	present	no	*P. albicaulis*
WW212	0.1 m, 27 cm	rooted stump	present	no	*P. albicaulis*
WW213	1.2 m, 30 cm	rooted stump	present	no	*P. albicaulis*
WW214	0.4 m, 25 cm	rooted stump	present	no	*P. albicaulis*
WW215	1.3 m, 27 cm	downed log	present	no	*P. lambertiana*
WW216	0.2 m, 31 cm	downed log	absent	no	*T. mertensiana*
WW217	7.2 m, 100 cm	downed log	present	no	*T. mertensiana*
WW218	8.2 m, 121 cm	downed log	present	no	yellow pine grp
WW219	1.3 m, 37 cm	rooted stump	present	no	*P. lambertiana*
WW220	0.2 m, 31 cm	rooted stump	present	no	*P. monticola*
Whitewing Mountain–North Summit Plateau:					
WW1–94	6 m, 43 cm	downed log	absent	yes	*P. contorta*
WW2–94	9 m, 41 cm	downed log	absent	yes	*P. contorta*
WW13–94	8 m, 41 cm	downed log	absent	yes	*P. contorta*
WW14–95	7 m, 39 cm	downed log	absent	yes	yellow pine grp
WW15–95	5 m, 32 cm	downed log	absent	yes	*P. lambertiana*
WW16–95	9 m, 78 cm	downed log	absent	yes	yellow pine grp
WW17–95	8 m, 55 cm	downed log	absent	yes	*P. albicaulis*
WW101–95	7 m, 58 cm	downed log	absent	yes	*P. monticola*
WW103–95	4 m, 45 cm	downed log	absent	yes	white pine grp
WW105–95	6 m, 45 cm	downed log	absent	yes	*P. monticola*
Whitewing Mountain–Central Summit Plateau:					
WW3–94	9 m, 43 cm	downed log	absent	yes	*P. jeffreyi*
WW4–94	6 m, 20 cm	downed log	absent	yes	*P. monticola*
WW5–94	3 m, 45 cm	downed log	absent	yes	*P. monticola*
WW11–94	0.3 m, 30 cm	upright stem	rooted	yes	*P. albicaulis*
WW12–94	7 m, 78 cm	downed log	absent	no	*P. jeffreyi*
WW18–95	8 m, 65 cm	downed log	absent	no	*P. albicaulis*

Appendix A (*continued*)

Sample ID	Stem Length and Diameter[a]	Condition	Stump	Dated?	Species ID[b]
Whitewing Mountain–Central Summit Plateau:					
WW19–95	5 m, 48 cm	downed log	absent	yes	*P. albicaulis*
WW20–95	6 m, 35 cm	downed log	absent	yes	yellow pine grp
WW21–95	3 m, 22 cm	downed log	absent	yes	*P. albicaulis*
WW106–95	4 m, 35 cm	downed log	absent	no	*P. monticola*
WW107–95	5 m, 42 cm	downed log	absent	no	*P. albicaulis*
WW108–95	2 m, 24 cm	downed log	absent	no	*P. albicaulis*
WW109–95	3 m, 35 cm	downed log	absent	yes	*P. albicaulis*
WW110–95	7 m, 80 cm	downed log	absent	no	*P. monticola*
WW111–95	6 m, 65 cm	downed log	absent	yes	*P. albicaulis*
WW112–95	4 m, 45 cm	downed log	absent	no	white pine grp
WW113–95	7 m, 75 cm	downed log	absent	no	*P. albicaulis*
WW114–95	4 m, 45 cm	downed log	absent	yes	*P. albicaulis*
WW115–95	7 m, 75 cm	downed log	absent	yes	*P. albicaulis*
WW116–95	6 m, 72 cm	downed log	absent	no	yellow pine group
WW509–98	1 m, 40 cm	upright stem	rooted	no	*P. albicaulis*
Whitewing Mountain–South Summit Plateau:					
WW6–94	5 m, 25 cm	downed log	absent	yes	*P. lambertiana*
WW7–94	1 m, 38 cm	upright stem	rooted	no	*P. albicaulis*
WW9–94	9 m, 43 cm	downed log	absent	yes	*P. monticola*
WW10–94	4 m, 28 cm	downed log	absent	yes	*P. albicaulis*
WW501–98	2 m, 35 cm	upright stem	rooted	yes	*P. albicaulis*
WW508–98	1 m, 37 cm	upright stem	rooted	no	*P. albicaulis*
Whitewing Mountain–West Summit Ridge:					
WW8–94	5 m, 32 cm	downed log	present	no	*P. albicaulis*
WW502–98	1 m, 36 cm	wood segment	absent	no	*P. albicaulis*
WW503–98	2 m, 27 cm	upright stem	rooted	yes	*P. albicaulis*
WW504–98	3 m, 36 cm	upright stem	rooted	yes	*P. albicaulis*
WW505–98	8 m, 42 cm	downed stem	absent	yes	*P. albicaulis*
San Joaquin Ridge:					
SJ1–98	9 m, 45 cm	downed log	present	no	*P. albicaulis*
SJ2–98	8 m, 43 cm	downed log	present	yes	*P. albicaulis*

(*continued on next page*)

Appendix A (*continued*)

Sample ID	Stem Length and Diameter[a]	Condition	Stump	Dated?	Species ID[b]
San Joaquin Ridge:					
SJ3–98	7 m, 30 cm	downed log	present	yes	*P. albicaulis*
SJ4–98	9 m, 38 cm	downed log	present	yes	*P. albicaulis*
SJ5–98	8 m, 40 cm	downed log	present	yes	*P. albicaulis*
SJ6–98	6 m, 35 cm	downed log	present	yes	*P. albicaulis*
SJ7–98	3 m, 22 cm	downed log	present	yes	*P. albicaulis*
SJ2–1–99	6 m, 50 cm	downed log	present	no	*P. albicaulis*
SJ2–2–99	1 m, 25 cm	downed log	present	no	*P. albicaulis*
SJ2–3–99	4 m, 30 cm	downed log	present	no	*P. albicaulis*
SJ2–4–99	2 m, 32 cm	downed log	present	yes	*P. albicaulis*
SJ2–5–99	3 m, 35 cm	downed log	present	no	*P. albicaulis*
SJ2–6–99	7 m, 45 cm	downed log	present	yes	*P. albicaulis*
SJ2–7–99	6 m, 38 cm	downed log	present	yes	*P. albicaulis*
SJ2–8–99	9 m, 43 cm	downed log	present	yes	*P. albicaulis*
SJ2–9–99	5 m, 39 cm	downed log	present	no	*P. albicaulis*
SJ2–10–99	8 m, 41 cm	downed log	present	yes	*P. albicaulis*

[a] Diameters of basal-most part of stem.
[b] White pine group includes *Pinus lambertiana*, *P. monticola* and *P. flexilis*, yellow pine group includes *P. jeffreyi, P. contorta,* and *P. ponderosa*.

References

Anderson, R.S., 1990. Holocene forest development and paleoclimates within the central Sierra Nevada, California. Journal of Ecology 78, 470–489.

Arundel, S.T., 2005. Using spatial models to establish climatic limiters of plant species' distributions. Ecological Modeling 182, 159–181.

Bailey, R.A., Dalrymple, G.B., Lanphere, M.A., 1976. Volcanism, structure, and geochronology of Long Valley Calder, Mono County, California. Journal of Geophysical Research 81, 725–744.

Benson, L., Kashgarian, M., Rye, R., Lund, S., Paillet, F., Smoot, J., Kester, C., Mensing, S., Meko, D., Lindstrom, S., 2002. Holocene multidecadal and multicentennial droughts affecting northern California and Nevada. Quaternary Science Reviews 21, 659–682.

Clark, D.H., Gillespie, A.R., 1997. Timing and significance of late-glacial and Holocene cirque glaciation in the Sierra Nevada, California. Quaternary Research 19, 117–129.

Cook, E.R., Holmes, R.L., 1992. Program CRONOL. In: Grissino-Mayer, H.D., Holmes, R.L., Fritts, H.C (Eds.), International Tree-Ring Data Bank Program Library, User's Manual. Laboratory of Tree-Ring Research, Tucson (AZ).

Cook, E.R., Kairukstis, L.A. (Eds.), 1990. Methods of Dendrochronology. Kluwer, Dordrecht, Netherlands, 394 pp.

Critchfield, W.B., Little, E.L., 1966. Geographic distribution of pines of the world. USDA Forest Service. Miscellaneous Publication, vol. 991. 97 pp.

Daly, C., Neilson, R.P., Phillips, D.L., 1994. A statistical-topographic model for mapping climatological precipitation over mountainous terrain. Journal of Applied Meteorology 33, 140–158 (http://www.orst.edu/prism/).

Davis, F.W., Stoms, D.M., Hollander, A.D., Thomas, K.A., Stine, P.A., Odion, D., Borchert, M.I., Thorne, J.H., Gray, M.V., Walker, R.E., Warner, K., Graae, J., 1998. The California Gap Analysis Project-Final Report. University of California, Santa Barbara, CA. http://www.biogeog.ucsb.edu/projects/gap/gap_rep.html.

Dettinger, M.D., Cayan, D.R., Meyer, M.K., Jeton, A.E., 2004. Simulated hydrologic responses to climate variation and change in the Merced, Carson, and American River basins, Sierra Nevada, California, 1900–2099. Climatic Change 62, 283–317.

Esper, J., Cook, E.R., Schweingruber, F.H., 2002. Low-frequency signals in long tree-ring chronologies for reconstructing past temperature variability. Science 295, 2250–2253.

ESRI (Environmental Systems Research Institute), 2002. ArcINFO: Release 8.3. Environmental Systems Research Institute, Redlands, California.

Fritts, H.C., 1976. Tree Rings and Climate. Academic Press, New York.

Graumlich, L.G., 1993. A 1000-yr record of temperature and precipitation in the Sierra Nevada. Quaternary Research 39, 249–255.

Graumlich, L.J., Lloyd, A.H., 1996. Dendroclimatic, ecological, and geomorphological evidence for long-term climatic change in the Sierra Nevada, USA. Radiocarbon 51–59.

Griffin, J.R., Critchfield, W.B., 1976. The distribution of forest trees in California. USDA Forest Service. Pacific Southwest Research Station Research Paper, vol. PSW-82. 114 pp.

Hamann, A., Wang, T.L., 2005. Models of climatic normals for genecology and climate change studies in British Columbia. Agricultural & Forest Meteorology 128, 211–221.

Hayhoe, K., Cayan, D., Field, C.B., 2004. Emissions pathways, climate change, and impacts on California. Proceedings of the National Academy of Science 101, 12422–12427.

Holmes, R.L., Adams, R.K., Fritts, H.C., 1986. Tree-ring chronologies of western North America: California, Eastern Oregon, and Northern Great Basin with procedures used in the chronology development work including user's manuals for computer programs COFECHA and ARSTAN. Laboratory of Tree-Ring Research, University of Arizona, Chronology Series VI.

IAWA, 2004. List of microscopic features for softwood identification. International Association of Wood Anatomists Journal 25, 1–70.

ITRDB (International Tree-Ring Data Bank), 2005a. IGBP PAGES/World Data Center for Paleoclimatology, NOAA/NCDC Paleoclimatology Program, Boulder, Colorado, USA. Chronology numbers Ca505 (C.W. Ferguson and M.C. Parker); Ca 567, Ca579, Ca 580, Ca606, Ca633, (J.C. King).

ITRDB (International Tree-Ring Data Bank), 2005b. IGBP PAGES/World Data Center for Paleoclimatology, NOAA/NCDC Paleoclimatology Program, Boulder, Colorado, USA. Chronology numbers Ca533 (D.A. Graybill and V.C. LaMarche); NV519, Ca605, Ca606, Ca633 (J.C. King).

ITRDB (International Tree-Ring Data Bank), 2005c. IGBP PAGES/World Data Center for Paleoclimatology, NOAA/NCDC Paleoclimatology Program, Boulder, Colorado, USA. Chronology numbers Ca561, Ca562, Ca563, Ca564, Ca566, Ca 567, Ca 568, Ca 569, Ca 570, Ca 571, Ca 572, Ca 573, Ca 574, Ca 575, Ca 576, Ca 578, Ca 579, Ca 580, Ca 581, Ca 582, Ca583, Ca 584, Ca 585, Ca 586, Ca 587, Ca 588, Ca 589, Ca 590, Ca 591, Ca 592, Ca 593, Ca 595, Ca 596, Ca 597, Ca 602, Ca 603, Ca 604, Ca 605, Ca 606, Ca 607 (J.C. King).

ITRDB (International Tree-Ring Data Bank), 2005d. IGBP PAGES/World Data Center for Paleoclimatology, NOAA/NCDC Paleoclimatology Program, Boulder, Colorado, USA. Chronology numbers Ca 528, Ca530, Ca535 (D.A. Graybill); Ca 533, (D.A. Graybill and V.C. LaMarche); Nv 519, Ca 605, Ca606, Ca633 (J.C. King); Ca630, Ca631 (D. Meko et al.).

Jackson, S.T., Overpeck, J.T., 2000. Responses of plant populations and communities to environmental changes of the late Quaternary. Paleobiology 25, 194–220.

Kellogg, R.M., Rowe, S., Koeppen, R.C., Miller, R.B., 1982. Identification of the wood of the soft pines of western North America. International Association of Wood Anatomists Bulletin 3, 95–101.

Kinloch, B.B., Scheuner, W.H., 1990. Sugar pine. In, Burns, Russell M., and Barbara H. Honkala, (eds.), Silvics of North America: 1. Conifers; 2. Hardwoods. Agriculture Handbook 654. U.S. Department of Agriculture, Forest Service, Washington, DC, vol.2.

Kleepe, J.A., in press. A study of ancient trees rooted 36.5 m (120′) below the surface level of Fallen Leaf Lake. Journal of Nevada Water Resources Association.

Konrad, S., Clark, D.H., 1998. Evidence for an early Neoglacial advance from rock glaciers and lake sediments in the Sierra Nevada, California, U.S.A. Arctic and Alpine Research 30, 272–284.

Kukachka, B.F., 1960. Identification of coniferous woods. Tappi 43, 887–896.

Li, H.C., Bischoff, J.L., Ku, T.L., Lund, S.P., Stott, L.D., 2000. Climate variability in East- Central California during the past 1000 years reflected by high-resolution geochemical and isotopic records from Owens Lake sediments. Quaternary Research 54, 189–197.

Lloyd, A.H., Graumlich, L.J., 1997. Holocene dynamics of the tree line forests in the Sierra Nevada. Ecology 78, 1199–1210.

Mann, M.E., Bradley, R.S., Hughes, M.K., 1999. Northern hemisphere temperatures during the past millennium: inferences, uncertainties, and limitations. Geophysical Research Letters 26, 759–762.

Meko, D.M., Therrell, M.D., Baisan, C.H., Hughes, M.K., 2001. Sacramento River flow reconstructed to AD 869 from tree rings. Journal of the American Water Resources Association 37, 1029–1040.

Millar, C.I., Westfall, R.D., Delany, D.L., King, J.C., Graumlich, L.C., 2004. Response of subalpine conifers in the Sierra Nevada, California, U.S.A., to 20th-century warming and decadal climate variability. Arctic, Antarctic, and Alpine Research 36, 181–200.

Miller, C.D., 1984. Chronology and stratigraphy of recent eruptions at the Inyo volcanic chain. Friends of the Pleistocene Field Trip Guide, October 12–14, 1983, 89–96.

Miller, C.D., 1985. Holocene eruptions at the Inyo volcanic chain, California—Implications for possible eruptions in the Long Valley Caldera. Geology 13 (1), 14–17.

Miller, R.B., Wiedenhoeft, A.C., 2003. Microscopic wood identification of *Pinus contorta* Engelm. and *Pinus ponderosa* Dougl. Ex Laws. IUFRO Congress in Rotorua, New Zealand. Abstract. Journal 24, 99.

SAS Institute Inc., 2004. SAS OnlineDoc® 9.1.2. Cary, NC: SAS Institute Inc. JMP Statistics and Graphics Guide, version 5. SAS Institute Inc., Cary, NC.

Scuderi, L., 1993. A 2,000-year record of annual temperatures in the Sierra Nevada Mountains. Science 259, 1433–1436.

Sieh, K., Bursik, M., 1986. Most recent eruption of the Mono Craters, Eastern Central California. Journal of Geophysical Research 91 (B12), 12,539–12,571.

Sorey, M.L., Evans, W.C., Kennedy, B.M., Farrar, C.D., Hainsworth, L.J., Hausback, B., 1998. Carbon dioxide and helium emissions from a reservoir of magmatic gas beneath Mammoth Mountain, California. Journal of Geophysical Research 103, 15303–15323.

Stine, S., 1990. Late Holocene fluctuations of Mono Lake, Eastern California. Palaeogeography, Palaeoclimatology, and Palaeoecology 78, 333–382.

Stine, S., 1994. Extreme and persistent drought in California and Patagonia during Medieval time. Nature 369, 546–549.

Stine, S., Wood, S., Sieh, K., Miller, C.D., Oct 12–14, 1984. Holocene paleoclimatology and tephrochronology east and west of the central Sierran crest. Fieldtrip Guidebook for Friends of the Pleistocene Pacific Cell.

Stokes, M.A., Smiley, T.L., 1968. An Introduction to Tree-Ring Dating. University of Chicago Press, Chicago, 73 pp.

Wiedenhoeft, A.C., Miller, R.B., Theim, T.J., 2003a. Analysis of three microscopic characters for separating the wood of *Pinus contorta* Engelm. and *Pinus ponderosa* Dougl. ex Laws. Journal 24, 257–267.

Wiedenhoeft, A.C., Miller, R.B., Knight, M., Berry, P.E., 2003b. Crystals in the resin canal complexes of *Pinus* as a character for pine systematics and wood identification [Abstract]. International Association of Wood Anatomists Journal 24, 333–334.

Wolfram Research, Inc., 2004. Mathematica. A system for doing mathematics by computer. Vs. 5.1. Champaign, IL.

Wood, S.H., 1977. Distribution, correlation, and radiocarbon dating of late Holocene tephra, Mono and Inyo craters, eastern California. Geological Society of America Bulletin 88, 89–95.

Woolfenden, W.B., 1996. Quaternary vegetation history. Sierra Nevada Ecosystem Project: Final Report to Congress, vol. II. University of California, Center for Water and Wildland Research, pp. 47–70.

WRCC (Western Regional Climate Center), 2005. Instrumental weather databases for western climate stations, data archived at: http://wrcc.dri.edu.

Yamaguchi, D.K., 1994. More on estimating the statistical significance of cross-dating positions for “floating” tree-ring series. Canadian Journal of Forest Research 24, 427–429.

Yamaguchi, D.K., Allen, G.A., 1992. A new computer program for estimating the statistical significance of cross-dating positions for “floating” tree-ring series. Canadian Journal of Forest Research 22, 1215–1221.

Yuan, F., Linsley, B.K., Lund, S.P., McGeehin, J.P., 2004. A 1200-year record of hydrologic variability in the Sierra Nevada from sediments in Walker Lake, Nevada. Geochemistry, Geophysics, Geosystems 5, 1–13.